PROCEEDINGS OF SPIE

SPIEDigitalLibrary.org/conference-proceedings-of-spie

Light-induced plasmonic properties of organic materials: surface polaritons, bistability and switching waves

Boris D. Fainberg
Nikolay N. Rosanov
Nikolay A. Veretenov
Boris Apter

SPIE.

Invited Paper

Light-induced "plasmonic" properties of organic materials: surface polaritons, bistability and switching waves

Boris D. Fainberg[a,b,c], Nikolay N. Rosanov [c,d,e], Nikolay A. Veretenov [c,d], Boris Apter[a]

[a]Holon Institute of Technology, 52 Golomb street, Holon 5810201, Israel
[b]Tel Aviv University, School of Chemistry, Tel Aviv 69978, Israel
[c]ITMO University, St. Petersburg 197101, Russia
[d]Vavilov State Optical Institute, St. Petersburg 199053, Russia
[e]Ioffe Physical-Technical Institute, St. Petersburg 194021, Russia

ABSTRACT

Purely organic materials with negative and near-zero dielectric permittivity can be easily fabricated, and propagation of surface polaritons at the material/air interface was demonstrated. Here we develop a mean-field theory of nonlinear light-induced "plasmonic" properties of organic materials. The theory describes both a red shift of the resonance frequency of isolated molecules, according to the Clausius-Mossotti Lorentz-Lorentz mechanism, and the wide variations of their spectra related to the aggregation of molecules into J- or H-aggregates. The bistable response of organic materials in the condensed phase has been demonstrated using the electron-vibrational model. We predict the generation of the switching waves, or kinks in the bistable organic thin films that enable us to observe a bistable behaviour of the surface polaritons at the organic thin film/dielectric interface under the laser irradiation. We present the alternating-sign dependence of the switching wave velocity on pump intensity and discuss a possibility of controlling the polariton propagation by switching waves.

Keywords: Organic "plasmonics", Surface polaritons, Bistability, Switching waves

1. INTRODUCTION

Plasmonics and metamaterials provide great scope for concentrating and manipulating the electromagnetic field on the subwavelength scale to achieve dramatic enhancement of optical processes and to develop super-resolution imaging, optical cloaking etc.[1–4] However, metallic inclusions in metamaterials are sources of strong absorption loss. This hinders many applications of metamaterials and plasmonics and motivates to search for efficient solutions to the loss problem.[5] Highly doped semiconductors[5,6] and doped graphene[7–9] can in principle solve the loss problem. However, the plasmonic frequency in these materials is an order of magnitude lower than that in metals making former most useful at mid-IR and THz regions. In this relation the question arises whether metal-free metamaterials and plasmonic systems, which do not suffer from excessive damping loss, can be realized in the visible range? With no doubts, inexpensive materials with such advanced properties can impact wide technological fields of nanoplasmonics and metamaterials.

Recently Noginov et al. demonstrated that purely organic materials characterized by low losses with negative, near-zero, and smaller than unity dielectric permittivities can be easily fabricated.[10] Specifically, the substantially strong negative dielectric permittivity demonstrated in zinc tetraphenylporphyrin (ZnTPP), suggests that this dye compound can function as a plasmonic material. The experimental demonstration of a surface plasmon polariton propagating at the ZnTPP/air interface has been realized.[10]

In addition, Gentile et al.[11] showed that polymer films doped with J-aggregated (TDBC) molecules might exhibit a negative real permittivity in the vicinity of the exciton resonance. Thin films of such material may support surface exciton-polariton modes, in much the same way that thin metal films support surface plasmon-polariton modes. Furthermore, they used the material parameters derived from experiment to demonstrate that nanostructured excitonic materials may support localized surface exciton-polariton modes.

Send correspondence to B.D.F.: E-mail: fainberg@hit.ac.il

Light Manipulating Organic Materials and Devices IV, edited by Manfred Eich, Jean-Michel Nunzi, Jon A. Schuller, Joy E. Haley, Proc. of SPIE Vol. 10360, 1036003 · © 2017 SPIE
CCC code: 0277-786X/17/$18 · doi: 10.1117/12.2272741

Moreover, near-zero dielectric permittivity of the organic host medium results in dramatic enhancement of intersite dipolar energy-transfer interaction in the quantum dot wire that influences on electron transport through nanojunctions.[12] Such interactions can compensate Coulomb repulsions in the wire for particular conditions.[12–14] And even the dramatic laser-induced change of the dielectric permittivity of dyes may be realized[12,15] that can enable us to control their "plasmonic" properties.

The results of both approaches[10] and[11] were explained in simple terms of the Lorentz model for linear spectra of dielectric permittivities of thin film dyes. However, the experiments with strong laser pulses[15] challenge theory. The point is that the Lorentz model based on a mean-field theory is described by essentially nonlinear equations for strong laser excitation. Their general solution is not a simple problem. In addition, such nonlinear equations can predict bistability etc.

Here we develop a theory of the light-induced "plasmonic" properties of organic materials. Our consideration is based on the model of the interaction of strong shaped laser pulse with organic molecules, Ref.,[16] extended to the dipole-dipole intermolecular interactions in the condensed matter. These latters are taken into account using a mean-field theory that resulted in two options: one mother - two daughters. The first option correctly describes the behaviour of the first moment of molecular spectra in condensed matter, and specifically, the red shift, according to the Clausius-Mossotti Lorentz-Lorentz (CMLL) mechanism.[17] The second option is related to the dramatic modification of molecular spectra in condensed matter due to the aggregation of molecules into J- or H-aggregates. Among other things we predict the bistable response of organic materials in the condensed phase. The phenomenon of bistability in spatially distributed systems acquires new important features well developed in optical bistability.[18,19] Among the key elements here are switching waves, or kinks responsible for such effects as spatial bistability, spatial hysteresis and dissipative solitons.[19] The goal of this study is also the search and investigation of the switching waves (SWs) in the organic "plasmonic" materials and discussion of their connection with the surface polaritons (SPs).

2. DERIVATION OF EQUATIONS FOR DIPOLE-DIPOLE INTERMOLECULAR INTERACTIONS IN CONDENSED MATTER

In this section we shall extend our picture of "moving" potentials of Ref.[16] to a condensed matter. In this picture we considered a molecule with two electronic states $n = 1$ (ground) and 2 (excited) in a solvent described by the Hamiltonian

$$H_0 = \sum_{n=1}^{2} |n\rangle \left[E_n + W_n(\mathbf{Q})\right] \langle n| \tag{1}$$

where $E_2 > E_1, E_n$ is the energy of state $n, W_n(\mathbf{Q})$ is the adiabatic Hamiltonian of reservoir R (the vibrational subsystems of a molecule and a solvent interacting with the two-level electron system under consideration in state n). The molecule is affected by electromagnetic field $\mathbf{E}(t)$

$$\mathbf{E}(t) = \frac{1}{2}\mathbf{e}\mathcal{E}(t)\exp(-i\omega t + i\varphi(t)) + \text{c.c.} \tag{2}$$

the frequency of which is close to that of the transition $1 \to 2$. Here $\mathcal{E}(t)$ and $\varphi(t)$ describe the change of the pulse amplitude and phase in time, $\mathbf{e}$ is unit polarization vector.

One can describe the influence of the vibrational subsystems of a molecule and a solvent on the electronic transition within the range of definite vibronic transition related to a high frequency optically active (OA) vibration as a modulation of this transition by low frequency (LF) OA vibrations $\{\omega_s\}$.[20] In accordance with the Franck-Condon principle, an optical electronic transition takes place at a fixed nuclear configuration. Therefore, the quantity $u_1(\mathbf{Q}) = W_2(\mathbf{Q}) - W_1(\mathbf{Q}) - \langle W_2(\mathbf{Q}) - W_1(\mathbf{Q})\rangle_1$ representing electron-vibration coupling is the disturbance of nuclear motion under electronic transition where $\langle\rangle_n$ stands for the trace operation over the reservoir variables in the electronic state n. Electronic transition relaxation stimulated by LFOA vibrations is described by the correlation function $K(t) = \langle\alpha(0)\alpha(t)\rangle$ of the corresponding vibrational disturbance with characteristic attenuation time τ_s[21–23] where $\alpha \equiv -u_1/\hbar$. The analytic solution of the problem under consideration has been obtained due to the presence of a small parameter. For broad vibronic spectra satisfying the "slow modulation" limit, we have $\sigma_{2s}\tau_s^2 \gg 1$ where $\sigma_{2s} = K(0)$ is the LFOA vibration contribution to a second central moment

of an absorption spectrum, the half bandwidth of which is related to σ_{2s} as $\Delta\omega_{abs} = 2\sqrt{2\sigma_{2s}\ln 2}$. According to Refs.,[22,23] the following times are characteristic for the time evolution of the system under consideration: $\sigma_{2s}^{-1/2} < T' << \tau_s$, where $\sigma_{2s}^{-1/2}$ and $T' = (\tau_s/\sigma_{2s})^{1/3}$ are the times of reversible and irreversible dephasing of the electronic transition, respectively. The characteristic frequency range of changing the optical transition probability can be evaluated as the inverse T', i.e. $(T')^{-1}$. Thus, one can consider T' as a time of the optical electronic transition. Therefore, the inequality $\tau_s \gg T'$ implies that the optical transition is instantaneous where relation $T'/\tau_s << 1$ plays the role of a small parameter.

This made it possible to describe vibrationally non-equilibrium populations in electronic states 1 and 2 by balance equations for the intense pulse excitation (pulse duration $t_p > T'$) and solve the problem.[16,24]

Let us include now the dipole-dipole intermolecular interactions in the condensed matter that are described by Hamiltonian[21,25] $H_{int} = \hbar \sum_{m \neq n} J_{mn} b_m^{\dagger} b_n$. Then Eq.(6) of Ref.[16] describing vibrationally non-equilibrium populations in electronic states $j = 1, 2$ for the exponential correlation function $K(t)/K(0) \equiv S(t) = \exp(-|t|/\tau_s)$ can be written as

$$\frac{\partial}{\partial t}\rho_{jj}(\alpha, t) = -i\hbar^{-1}[H_0(\alpha, t) + H_{int} - \mathbf{D}\cdot\mathbf{E}(t), \rho(\alpha, t)]_{jj} + L_{jj}\rho_{jj}(\alpha, t) \tag{3}$$

where $j = 1, 2$; and the operator L_{jj} is determined by the equation:

$$L_{jj} = \tau_s^{-1}\left[1 + (\alpha - \delta_{j2}\omega_{st})\frac{\partial}{\partial(\alpha - \delta_{j2}\omega_{st})} + \sigma_{2s}\frac{\partial^2}{\partial(\alpha - \delta_{j2}\omega_{st})^2}\right], \tag{4}$$

describes the diffusion with respect to the coordinate α in the corresponding effective parabolic potential $U_j(\alpha)$, δ_{ij} is the Kronecker delta, $\omega_{st} = \beta\hbar\sigma_{2s}$ is the Stokes shift of the equilibrium absorption and luminescence spectra, $\beta = 1/k_B T$. In the absence of the dipole-dipole intermolecular interactions in the condensed matter, H_{int}, Eq.(3) is reduced to Eq.(11) of Ref.[16] The partial density matrix of the system $\rho_{jj}(\alpha, t)$ describes the system distribution in states 1 and 2 with a given value of α at time t. The complete density matrix averaged over the stochastic process which modulates the system energy levels, is obtained by integration of $\rho_{ij}(\alpha, t)$ over α, $\langle\rho\rangle_{ij}(t) = \int \rho_{ij}(\alpha, t)\, d\alpha$, where quantities $\langle\rho\rangle_{jj}(t)$ are the normalized populations of the corresponding electronic states: $\langle\rho\rangle_{jj}(t) \equiv n_j$, $n_1 + n_2 = 1$. Knowing $\rho_{jj}(\alpha, t)$, one can calculate the positive frequency component of the polarization $\mathbf{P}^{(+)}(t) = N\mathbf{D}_{12}\langle\rho\rangle_{21}(t)$, and the susceptibility $\chi(\Omega, t)$[16] that enables us to obtain the dielectric function ε due to relation $\varepsilon(\Omega, t) = 1 + 4\pi\chi(\Omega, t)$. Here N is the density of molecules. It is worthy to note that magnitude $\varepsilon(\Omega, t)$ does make sense, since it changes in time slowly with respect to dephasing. In other words, $\varepsilon(\Omega, t)$ changes in time slowly with respect to reciprocal characteristic frequency domain of changing $\varepsilon(\Omega)$.

Consider the contribution of Hamiltonian $\hat{H}_{int}$ to the change of $\rho_{ij}(\alpha, t)$ in time. In other words, we shall generalize Eq.(11) of Ref.[16] to the dipole-dipole intermolecular interactions in the condensed matter. Using the Heisenberg equations of motion, one obtains that $\hat{H}_{int}$ gives the following contribution to the change of the expectation value of excitonic operator b_k in time

$$\frac{d}{dt}\langle b_k\rangle \sim \frac{i}{\hbar}\langle[\hat{H}_{int}, b_k]\rangle \equiv \frac{i}{\hbar}Tr([\hat{H}_{int}, b_k]\rho) = -i\sum_{n \neq k} J_{kn}\langle(\hat{n}_{k1} - \hat{n}_{k2})b_n\rangle \tag{5}$$

where $\hat{n}_{k1} = b_k b_k^{\dagger}$, and $\hat{n}_{k2} = b_k^{\dagger} b_k$ is the exciton population operator. Considering an assembly of identical molecules, one can write $\langle b_k\rangle = \rho_{21}(\alpha, t)$[26] if averaging in Eq.(5) is carried out using density matrix $\rho(\alpha, t)$. Consider the expectation value $\langle(\hat{n}_{k1} - \hat{n}_{k21})b_n\rangle = Tr[(\hat{n}_{k1} - \hat{n}_{k2})b_n\rho(\alpha_k, \alpha_n, t)]$ for $n \neq k$ where α_m is the effective vibrational coordinate of a molecule m ($m = k, n$). Due to fast dephasing (see above), it makes sense to neglect all correlations among different molecules,[21] and set $\langle(\hat{n}_{k12} - \hat{n}_{k2})b_n\rangle = \langle\hat{n}_{k1} - \hat{n}_{k2}\rangle\langle b_n\rangle$ and correspondingly $\rho(\alpha_k, \alpha_n, t) \simeq \rho(\alpha_k, t)\rho(\alpha_n, t)$, i.e. density matrix $\rho(\alpha_k, \alpha_n, t)$ is factorized. Here from dimension consideration one expectation value should be calculated using density matrix $\rho(\alpha, t)$, and another one - using $\langle\rho\rangle(t) = \int \rho(\alpha, t)\, d\alpha$. Since we sum with respect to n, it would appear reasonable to integrate with respect to α_n. However, this issue is not so simple. The point is that in addition to intramolecular vibrations, there is a

contribution of low-frequency intermolecular and solvent coordinates into effective coordinate α. Because of this, partitioning the vibrations into α_k and α_n groups is ambiguous, and the mean-field approximation gives two options[12]

$$p\langle b\rangle\langle\hat{n}_1-\hat{n}_2\rangle=\begin{pmatrix} p\rho_{21}(\alpha,t)\,\Delta n \\ p\langle\rho_{21}\rangle(t)\Delta'(\alpha,t)\end{pmatrix} \tag{6}$$

where $\Delta'(\alpha,t)=\rho_{11}(\alpha,t)-\rho_{22}(\alpha,t)$, $p\equiv-\sum_{n\neq k}J_{kn}$, $\Delta n\equiv n_1-n_2$. Below we shall discuss which option better corresponds to a specific experimental situation. Consideration based on non-equilibrium Green functions (GF) shows that the terms $p\rho_{21}(\alpha,t)$ and $p\langle\rho_{21}\rangle(t)$ on the right-hand-side of Eq.(6) represent the self-energy, $\Sigma_{21}(t)$, and the terms Δn and $\Delta'(\alpha,t)$ - the difference of the "lesser" GFs for equal time arguments, $G^<_{11}(t,t)-G^<_{22}(t,t)$, that are the density matrix, i.e. $p\langle b\rangle\langle\hat{n}_1-\hat{n}_2\rangle=\Sigma_{21}(t)[G^<_{11}(t,t)-G^<_{22}(t,t)]$. In other words, for the first line on the right-hand-side of Eq.(6), the self-energy depends on α and the "lesser" GFs $G^<_{11}(t,t)-G^<_{22}(t,t)$ do not. In contrast, for the second line on the right-hand-side of Eq.(6), the self-energy does not depend on α and the "lesser" GFs $G^<_{11}(\alpha;t,t)-G^<_{22}(\alpha;t,t)$ do depend. This yields $\partial\rho_{21}(\alpha,t)/\partial t\sim i\Sigma_{21}(t)[G^<_{11}(t,t)-G^<_{22}(t,t)]$. Adding term "$i\Sigma_{21}(t)[G^<_{11}(t,t)-G^<_{22}(t,t)]$" to the right-hand side of Eq.(9) of Ref.,[16] and using the procedure described there, we get the extension of Eq.(11) of Ref.[16] to the dipole-dipole intermolecular interactions in the condensed matter

$$\frac{\partial\rho_{jj}(\alpha,t)}{\partial t}=L_{jj}\rho_{jj}(\alpha,t)+\frac{(-1)^j\pi}{2}\Delta'(\alpha,t)\begin{pmatrix}\delta[\omega_{21}-p\Delta n-\omega-\alpha]|\Omega_R(t)|^2\\ \delta(\omega_{21}-\omega-\alpha)\,|\Omega_{eff}(t)|^2\end{pmatrix} \tag{7}$$

where $\Omega_R(t)=(\mathbf{D}_{12}\cdot\mathbf{e})\mathcal{E}(t)/\hbar$ is the Rabi frequency, $\mathbf{D}_{12}$ is the electronic matrix element of the dipole moment operator, $\Omega_{eff}(t)=\Omega_R(t)+2p\langle\rho_{21}\rangle(t)=\Omega_R(t)+2\Sigma_{21}(t)$ is the effective Rabi frequency that can be written as

$$\Omega_{eff}(t)=\frac{\Omega_R(t)}{1+p\int d\alpha\Delta'(\alpha,t)\,\zeta(\omega-\omega_{21}+\alpha)}, \tag{8}$$

Here $\int d\alpha\Delta'(\alpha,t)\,\zeta(\omega-\omega_{21}+\alpha)/\pi$ is the line-shape function that is reduced to that of a monomer molecule in the absense of the dipole-dipole interactions for the equilibrium value of $\Delta'(\alpha,t)$, $\zeta(\omega-\omega_{21}+\alpha)=\frac{P}{\omega-\omega_{21}+\alpha}-i\pi\delta(\omega-\omega_{21}+\alpha)$, P is the symbol of the principal value.

As one can see from Eq.(7), self-energy $\Sigma_{21}(t)=p\rho_{21}(\alpha,t)$ (the first line on the right-hand side of Eq.(6)) results in the frequency shift of spectra "$-p\Delta n$" without changing the line shapes.[12] One can show that this approach correctly describes the change of the first moment of optical spectra in the condensed matter. Calculations of p for isotropic medium give $p=\frac{4\pi}{3\hbar}|D_{12}|^2N>0$[12,21,27] that corresponds to a red shift, according to the Clausius-Mossotti Lorentz-Lorentz (CMLL) mechanism.[17] In contrast, self-energy $\Sigma_{21}(t)=p\langle\rho_{21}\rangle(t)$ (the second line on the right-hand-side of Eq.(6)) results in the change of both the frequency shift of spectra and their lineshapes. In that case considering the dense collection of molecules under the action of one more (weak) field

$$\tilde{\mathbf{E}}(t)=\frac{1}{2}\mathbf{e}\tilde{\mathcal{E}}(t)\exp(-i\Omega t)+\text{c.c.},$$

one gets for the positive frequency component of the polarization $\mathbf{P}^+=N\mathbf{D}_{12}\langle\rho_{21}\rangle(t)$

$$\mathbf{P}^+(\Omega,t)=-\frac{1}{3\hbar}N\mathbf{D}_{12}\frac{(\mathbf{D}_{21}\cdot\mathbf{e})\tilde{\mathcal{E}}(t)/2}{[\int d\alpha\Delta'(\alpha,t)\,\zeta(\Omega-\omega_{21}+\alpha)]^{-1}+p}, \tag{9}$$

for the susceptibility

$$\chi(\Omega,t)=-\frac{N|D_{12}|^2}{3\hbar}\frac{\int d\alpha\Delta'(\alpha,t)\,\zeta(\Omega-\omega_{21}+\alpha)}{1+p\int d\alpha\Delta'(\alpha,t)\,\zeta(\Omega-\omega_{21}+\alpha)} \tag{10}$$

and the dielectric function

$$\varepsilon(\Omega,t)=1-4\pi\frac{N|D_{12}|^2}{3\hbar}\frac{\int d\alpha\Delta'(\alpha,t)\,\zeta(\Omega-\omega_{21}+\alpha)}{1+p\int d\alpha\Delta'(\alpha,t)\,\zeta(\Omega-\omega_{21}+\alpha)} \tag{11}$$

It is worthy to note that the approximation of broad vibronic spectra underlying Eq.(7) can break down in the case of the formation of J-aggregates possessing rather narrow spectra. In such a case one should use more general theory that is not based on the approximation of broad vibronic spectra (see below).

Integration of Eq.(7) is achieved by the Green's function[24]

$$G_{jj}\left(\alpha,t;\alpha',t'\right)=\left[2\pi\sigma\left(t-t'\right)\right]^{-1/2}\exp\{-[(\alpha-\delta_{j2}\omega_{st}) \\ -\left(\alpha'-\delta_{j2}\omega_{st}\right)S\left(t-t'\right)]^{2}/\left(2\sigma\left(t-t'\right)\right)\} \tag{12}$$

where $\sigma\left(t-t'\right)=\sigma_{2s}\left[1-S^{2}\left(t-t'\right)\right]$, for the initial condition,

$$\rho_{jj}^{(0)}\left(\alpha\right)\equiv\rho_{jj}\left(\alpha,t=0\right)=\delta_{j1}\left(2\pi\sigma_{2s}\right)^{-1/2}\exp[-\alpha^{2}/\left(2\sigma_{2s}\right)] \tag{13}$$

We obtain

$$\rho_{jj}\left(\alpha,t\right)=\rho_{jj}^{(0)}\left(\alpha\right)+\left(-1\right)^{j}\frac{\pi}{2}\int_{0}^{t}dt' \\ \times\left(\begin{array}{c}|\Omega_{R}(t')|^{2}\Delta'\left(\omega_{21}-p\Delta n-\omega,t'\right)G_{jj}\left(\alpha,t;\omega_{21}-p\Delta n-\omega,t'\right)\\ |\Omega_{eff}(t')|^{2}\Delta'\left(\omega_{21}-\omega,t'\right)G_{jj}\left(\alpha,t;\omega_{21}-\omega,t'\right)\end{array}\right) \tag{14}$$

where $\Delta'\left(\omega_{21}-p\Delta n-\omega,t'\right)$ and $\Delta'\left(\omega_{21}-\omega,t'\right)$ satisfy nonlinear integral equations that can be easily obtained from Eq.(14). Integrating both sides of Eq.(14) with respect to α and bearing in mind that $\int_{-\infty}^{\infty}G_{jj}\left(\alpha,t;\omega_{21}-\omega\left(t'\right),t'\right)d\alpha=1$, we get

$$\frac{dn_{j}}{dt}=\left(-1\right)^{j}\frac{\pi}{2}\left(\begin{array}{c}|\Omega_{R}(t)|^{2}\Delta'\left(\omega_{21}-p\Delta n-\omega,t\right)\\ |\Omega_{eff}(t)|^{2}\Delta'\left(\omega_{21}-\omega,t\right)\end{array}\right) \tag{15}$$

2.1 Fast vibrational relaxation

Let us consider the particular case of fast vibrational relaxation when one can put the normalized correlation function $S\left(t-t'\right)\equiv K\left(t-t'\right)/K\left(0\right)$ equal to zero. Physically it means that the equilibrium distributions into the electronic states have had time to be set during changing the pulse parameters. Bearing in mind that for fast vibronic relaxation

$$\Delta'\left(\alpha,t\right)=\frac{n_{1}\left(t\right)}{\left(2\pi\sigma_{2s}\right)^{1/2}}\exp(-\frac{\alpha^{2}}{2\sigma_{2s}})-\frac{n_{2}\left(t\right)}{\left(2\pi\sigma_{2s}\right)^{1/2}}\exp[-\frac{\left(\alpha-\omega_{st}\right)^{2}}{2\sigma_{2s}}], \tag{16}$$

substituting the last equation into Eq.(15) and using Eq.(8), one gets

$$\frac{dn_{j}}{dt}=\left(-1\right)^{j}\tilde{J}(t)\sigma_{a}\,\mathrm{Re}\left(\begin{array}{c}n_{1}W_{a}(\omega+p\Delta n)-n_{2}W_{f}(\omega+p\Delta n)\\ \frac{n_{1}W_{a}(\omega)-n_{2}W_{f}(\omega)}{1-ip\pi[n_{1}W_{a}(\omega)-n_{2}W_{f}(\omega)]}\end{array}\right)-\left(-1\right)^{j}\frac{n_{2}}{T_{1}} \tag{17}$$

where $n_{1}+n_{2}=1$, σ_{a} is the cross section at the maximum of the absorption band, $\tilde{J}(t)$ is the power density of exciting radiation, and we added term "$\left(-1\right)^{j}n_{2}/T_{1}$" taking the lifetime T_{1} of the excited state into account. Here $-iW_{a(f)}(\omega)$ is the line-shape function of a monomer molecule for the absorption (fluorescence) for fast vibronic relaxation,

$$\int_{-\infty}^{\infty}d\alpha\Delta'\left(\alpha,t\right)\zeta(\omega-\omega_{21}+\alpha)/\pi=-i[n_{1}\left(t\right)W_{a}(\omega)-n_{2}\left(t\right)W_{f}(\omega)] \tag{18}$$

The imaginary part of "$-iW_{a(f)}(\omega)$" with sign minus, $-\,\mathrm{Im}[-iW_{a(f)}(\omega)]=\mathrm{Re}\,W_{a(f)}(\omega)\equiv F_{a(f)}(\omega)$, describes the absorption (fluorescence) lineshapes of a monomer molecule, and the real part, $\mathrm{Re}[-iW_{a(f)}(\omega)]=\mathrm{Im}\,W_{a(f)}(\omega)$, describes the corresponding refraction spectra.

It is worthy to note that although the above consideration was based on the "slow modulation" limit, the balance equations for the fast vibrational relaxation in the form of Eq.(17) is also correct in more general case when the "slow modulation" limit breaks down (see below).

2.2 LINE-SHAPE IN THE FAST VIBRATIONAL RELAXATION LIMIT

As a matter of fact, the real part of the expressions in the brackets of the first term on the right-hand side of Eq.(17) describes absorption and emission of molecules susceptible to the dipole-dipole intermolecular interactions expressed through their monomer spectra W_a and W_f. In particular case of weak radiation when $n_1 = 1$ and $n_2 = 0$, the second line of the brackets recovers the coherent exciton scattering (CES) approximation.[28–30] The latter is well suited to describe absorption spectra of both J- and H-aggregates using their monomer spectra and the intermolecular interaction strength that is a fitting parameter. As to describing absorption spectra of H-aggregates, one should take into account also high frequency OA intramolecular vibrations,[29] in addition to the LFOA vibrations $\{\omega_s\}$ under consideration in our paper. The general form of Eq.(17) enables us to do this.

It is worthy to note that the CES approximation describes well the shape of the absorption spectra of H-aggregates. However, the spectra calculated in the CES approximation are blue shifted with respect to experimental ones.[29] To resolve the problem, the authors of Ref.[29] empirically introduce additional red shift that can be understood in the context of our more general theory as the red shift due to the CMLL mechanism. For example, the frequency dependent "lesser" GFs corresponding to the CES approximation describe well the spectra of H-aggregates. The latters can interact with each other by dipole-dipole interaction leading to the CMLL red shift that is described by the frequency dependent self-energy. By this means, both mechanisms presented by the expressions in the brackets of the first term on the right-hand side of Eq.(17) may be important.

Furthermore, for the "slow modulation" limit,

$$W_{a(f)}(\omega) = \sqrt{\frac{1}{2\pi\sigma_{2s}}}\, w\Big(\frac{\omega - \omega_{21} + \delta_{a(f),f}\omega_{st}}{\sqrt{2\sigma_{2s}}}\Big) \tag{19}$$

where $w(z) = \exp(-z^2)[1 + i\,\mathrm{erf}\, i(z)]$ is the probability integral of a complex argument,[31] and

$$F_{a(f)}(\omega) = \sqrt{\frac{1}{2\pi\sigma_{2s}}}\, \exp[-\frac{\big(\omega_{21} - \omega - \delta_{a(f),f}\omega_{st}\big)^2}{2\sigma_{2s}}] \tag{20}$$

However, the Gaussian shape of the absorption spectrum obtained in the "slow modulation" limit is correct only near the absorption maximum. The wings decline much slower as $(\omega_{21} - \omega)^{-4}$.[32] At the same time, the second line in the brackets of the first term on the right-hand side of Eq.(17) describing absorption and emission of molecules susceptible to the dipole-dipole intermolecular interactions has a pole, giving strong absorption or emission, when $1/(p\pi) = n_2\,\mathrm{Im}\, W_f(\omega) - n_1\,\mathrm{Im}\, W_a(\omega)$. If parameter of the dipole-dipole intermolecular interaction p is rather large, the pole may be at a large distance from the absorption band maximum where the "slow modulation" limit breaks down. This means one should use exact expression for the monomer spectra W_a and W_f that are not limited by "slow modulation" approximation, and properly describe both the central spectra region and their wings. The exact calculation of the vibrationally equilibrium monomer spectra for the Gaussian-Markovian modulation with the exponential correlation function $S(t) = \exp(-|t|/\tau_s)$ gives[32,33] (see Appendix A)

$$W_{a(f)}(\omega) = \frac{\tau_s}{\pi}\, \frac{\Phi(1, 1 + x_{a(f)}; \sigma_{2s}\tau_s^2)}{x_{a(f)}} \tag{21}$$

where $x_{a(f)} = \tau_s/(2T_1) + \sigma_{2s}\tau_s^2 + i\tau_s(\omega_{21} - \omega - \delta_{a(f),f}\omega_{st})$, $\Phi(1, 1 + x_{a(f)}; \sigma_{2s}\tau_s^2)$ is a confluent hypergeometric function.[31]

Figs.1 and 2 show the calculation results of the absorption spectra of J-aggregates according to formula $\mathrm{Re}\{W_a(\omega)/[1 - ip\pi W_a(\omega)]\}$ obtained from the second line of the brackets of the first term on the right-hand side of Eq.(17) for $n_1 = 1$ and $n_2 = 0$, and their comparison with the monomer spectra $W_a(\omega)$. The spectra of Fig.1 correspond to a dense collection of molecules ($N = 10^{21} cm^{-3}$, Ref.[10]) with parameters close to those of molecule LD690:[16] $\sqrt{\sigma_{2s}} = 546\ cm^{-1}$, $\tau_s = 10^{-13} s$, $D_{12} = 10^{-17}$ CGSE that gives $\omega_{st} = 1420\ cm^{-1}$, $p = 2107\ cm^{-1}$. We put $T_1 = 10^{-9} s$.

One can see that in spite of strong narrowing the J-aggregate spectra with respect to those of monomers, the vibrations still give rather important contribution to broadening the J-aggregate spectra that may be crucial. Indeed, the half bandwidth of the J-aggregate absorption spectrum is about $3 \cdot 10^{12}\ rad/s$ that may far exceed the

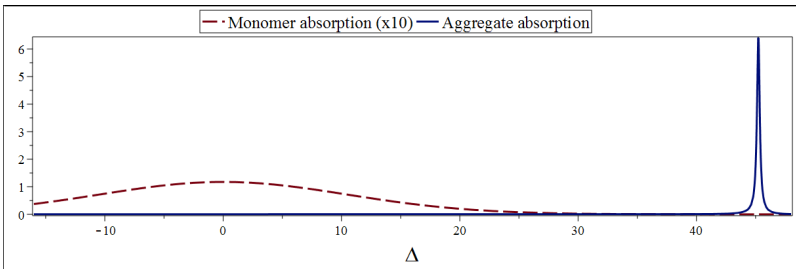

Figure 1. Absorption spectra of the J-aggregate (solid line) and the corresponding monomer (dotted line) in the case of slow modulation ($\sqrt{\sigma_{2s}}\tau_s = 10.9 >> 1$). Dimensionless parameter is $\Delta = \tau_s(\omega_{21} - \omega)$.

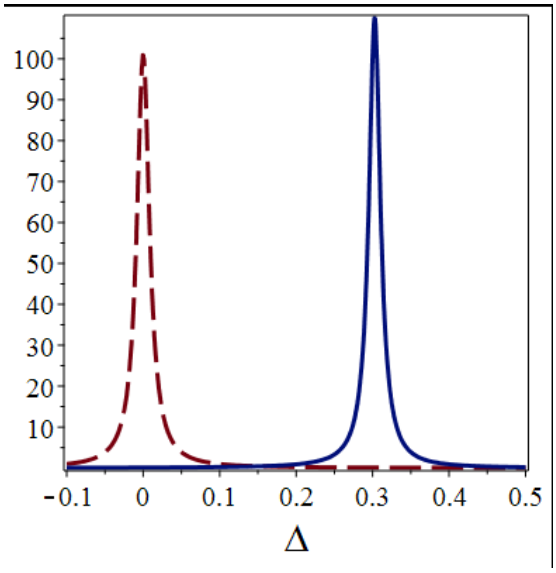

Figure 2. Absorption spectra of the J-aggregate (solid line) and the corresponding monomer (dotted line) in the case of fast modulation ($\sqrt{\sigma_{2s}}\tau_s = 0.1 << 1$) for $p\tau_s = 0.3$.

lifetime contribution. So, disregarding vibrations in the description of the J-aggregate spectra may be incorrect. In contrast, the J-aggregate absorption spectrum calculated using the monomer spectrum W_a, Eq.(19), and, as a consequence, the Gaussian absorption spectrum, Eq.(20), is extremely narrow (see also[30]).

In the case of fast modulation when $\sigma_{2s}\tau_s^2 << 1$, the aggregate spectrum only shifts with respect to the monomer one almost without changing its shape (Fig.2). Indeed, $\Phi(1, 1 + x_{a(f)}; \sigma_{2s}\tau_s^2) \approx 1$ for $\sigma_{2s}\tau_s^2 << 1$. In that case $W_{a(f)}(\omega) \approx (\tau_s/\pi)/x_{a(f)}$, and the spectral broadening becomes $\sigma_{2s}\tau_s = \omega_{st}\frac{\tau_s}{\beta\hbar} >> \omega_{st}$, since $\frac{\tau_s}{\beta\hbar} >> 1$ in the high-tmperature limit. In that case one can neglect ω_{st} in comparison with the spectral bandwidth so that $x_a \approx x_f$ and $W_f(\omega) \approx W_a(\omega)$. In that case the second line of the brackets of the first term on the right-hand side of Eq.(17) becomes

$$\mathrm{Re}\,\frac{n_1 W_a(\omega) - n_2 W_f(\omega)}{1 - ip\pi[n_1 W_a(\omega) - n_2 W_f(\omega)]} \approx \frac{1}{\pi}\,\mathrm{Re}\,\frac{\Delta n}{\frac{1}{2T_1} + \sigma_{2s}\tau_s + i(\omega_{21} - \omega - p\Delta n)} = \Delta n W_a(\omega + p\Delta n) \qquad (22)$$

In other words, if the monomer spectrum has Lorentzian shape, the aggregate spectrum is simply shifted monomer spectrum. This conclusion can be considered as the extension of the corresponding conclusion of Ref.[30] to non-equilibrium case when $\Delta n \neq 1$. It is worthy to note that for the Lorentzian monomer spectrum both lines of the brackets of the first term on the right-hand side of Eq.(17) coincide.

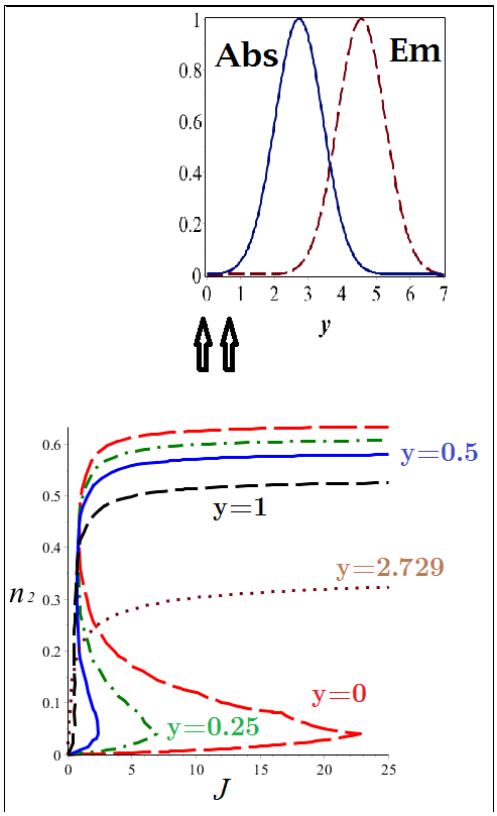

Figure 3. (Color online) Dependence of excited state population n_2 on power density of the exciting radiation $\tilde{J}$ at different detunings $\omega_{21}-\omega$. Dimensionless parameters are $J=\sigma_a\tilde{J}T_1$ and $y=(\omega_{21}-\omega)/\sqrt{2\sigma_{2s}}$. Parameters $\sqrt{\sigma_{2s}}$, ω_{st} and p are identical to those of Section2.2. Inset: Equilibrium spectra of the absorption (Abs) and the emission (Em); the arrows limit the frequency interval where calculated excited state populations n_2 show bistability.

3. BISTABILITY

Eqs. (7) and (17) for populations are nonlinear equations and can demonstrate a bistable behavior. Consider first the CMLL mechanism of the dipole-dipole intermolecular interactions leading to the red shift (the first line in the brackets of the first term on the right-hand side of Eq.(17)) when one can use Eqs.(19)-(20) for the monomer spectra. Fig.3 shows steady-state solutions of Eq.(17) for n_2 as a function of the power density of the exciting radiation $\tilde{J}$ at different detunings $\omega_{21}-\omega$. One can see that each value of $\tilde{J}$ within the corresponding interval produces three different solutions of Eq.(17) for dimensionless detunings $y=(\omega_{21}-\omega)/\sqrt{2\sigma_{2s}}=0$, 0.25 and 0.5, however, only lower and upper branches are stable.[34] Such detunings correspond to the excitation at the short-wave part of the equilibrium absorption spectrum (see the Inset to Fig.3). As the excited state population increases, the spectrum exhibits the blue shift (see Eq.(17), the first line in the brackets) that should essentially contribute to the absorption. As a matter of fact, the bistable behavior of the population arises from the dependence of the resonance frequency of the molecules in dense medium on the number of excited molecules. In contrast, larger $y=1$, 2.729 correspond to the excitation closer to the central part of the equilibrium absorption spectrum. In that case the blue shift produces lesser increasing the absorption and even can decrease it (for $y=2.729$), so that the bistable behavior disappears.

4. SURFACE POLARITONS AND SWITCHING WAVES IN BISTABLE ORGANIC THING FILMS

As we noted in the introduction, the phenomenon of bistability in spatially distributed systems acquires new important features like as SWs, or kinks responsible for spatial bistability, spatial hysteresis and dissipative

solitons.[19] This section is devoted to the search and investigation of the SWs in the organic "plasmonic" materials and discussion of their connection with the SPs.

As before we consider molecules with two electronic states $n = 1$ (ground) and 2 (excited) in a solvent. The molecules are affected by radiation of power density $\tilde{J}$, the frequency of which is close to that of the transition $1 \rightarrow 2$. In the case of fast vibrational relaxation the dielectric function at frequency Ω can be written as[12]

$$\begin{aligned} \varepsilon(\Omega) &= 1 + i\frac{4\pi^{3/2}|D_{12}|^2 N}{3\hbar\sqrt{2\sigma_{2s}}} \sum_{j=1,2} (-1)^{j+1} n_j(t) \\ &\times w\left(\frac{\Omega - \omega_{21} + p\Delta n + \delta_{2j}\omega_{st}}{\sqrt{2\sigma_{2s}}}\right) \end{aligned} \tag{23}$$

for the CMLL red shift in condensed matter where we used Eq.(19). The excited state population n_2 obeys nonlinear Eq.(17) where we take into account only the first line of the brackets of the first term on the right-hand side of the equation that may be written as (see also[12]):

$$dn_2/dt = -F(n_2) \tag{24}$$

where

$$\begin{aligned} F(n_2) &= \frac{n_2}{T_1}\{[1 + \exp(-\frac{\hbar(\omega_{st} - 2\Delta\omega)}{2k_B T})]J \\ &\times \exp(-\frac{\Delta\omega^2}{2\sigma_{2s}}) + 1\} - J\exp(-\frac{\Delta\omega^2}{2\sigma_{2s}}), \end{aligned} \tag{25}$$

$\Delta\omega = (\omega_{21} - \omega) - p(1 - 2n_2)$, $J = \sigma_a \tilde{J} T_1$.

Since $\varepsilon(\Omega)$ depends on the electronic state populations n_j, the bistable behaviour of the population results in the bistable behavior of $\varepsilon(\Omega)$. Fig.4 shows the real part of $\varepsilon(\Omega)$, ε', for $(\Omega - \omega_{21})/\sqrt{2\sigma_{2s}} = -1.842$ calculated using Eq.(23), as a function of the power density of the exciting radiation related to the corresponding curve for the excited state population n_2 of Fig.3 at dimensionless detuning $(\omega_{21} - \omega)/\sqrt{2\sigma_{2s}} = 0.25$. The lower and upper branches of the curve for ε' correspond to the lower and upper stable branches, respectively, of the curve for n_2 in Fig.3. Indeed, the excitation of SPs at the organic thin film/air interface is possible for substantially strong negative values of dielectric function $\varepsilon(\Omega)$,[10,35] and therefore only the lower branch will correspond to the SP generation. In this relation the following question arises: how can one observe a bistable behaviour of SPs at the organic thin film/air interface under the laser irradiation? This can be achieved with the aid of transverse phenomena such as SWs, known in optical bistability.[19] The SWs were initiated by radiation heating the semiconductor rod. The point is that the absorption coefficient of a semiconductor increases with temperature. A similar dependence of the absorption coefficient of the molecules in dense medium on the power density of exciting radiation can be realized on the excitation at the blue side of the absorption spectrum (see Section 3). Because of this, one can expect the generation of SWs also in the organic films under consideration, though the mechanism of bistability is essentially different from that of a semiconductor.

Let us suppose that the organic thin film is irradiated with a strong field (pump) falling perpendicular to its surface (and the coordinate x that is parallel to the film surface), Fig.5. The point is that in the case of bistability, the steady-state distribution of the excited state population n_2 may be inhomogeneous with respect to x at the definite value of the power density of exciting radiation $\tilde{J}$ named the Maxwell value $\tilde{J}_M$,[19] even though $\tilde{J}$ does not depend on x (plane wave). For an arbitrary value of $\tilde{J}$, the distributions under discussion become non-steady-state ones resulting in the SWs.[19] In our case the SW will be related to the excitation (population n_2) profile propagating along the organic film. To analyze such SWs, we should take the excitation transfer along the organic film due to intermolecular interactions into account. Using phenomenological diffusional approach[36] and Eq.(24), one can write

$$\frac{\partial n_2}{\partial t} = D\frac{\partial^2 n_2}{\partial x^2} - F(n_2) \tag{26}$$

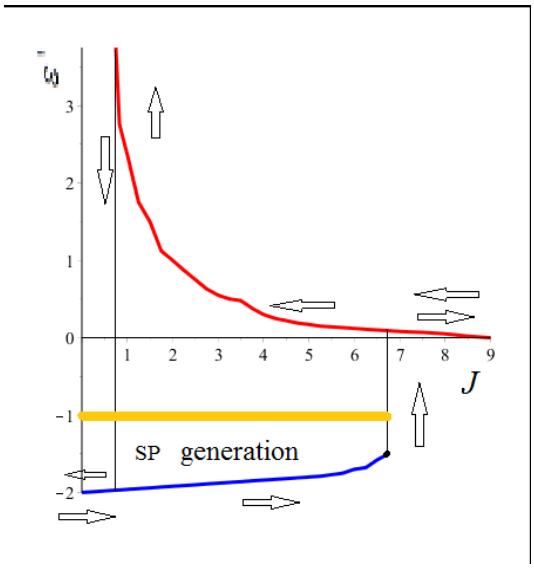

Figure 4. (Color online) Dependence of ε' on power density of the exciting radiation $\tilde{J}$ for $\varepsilon_b = 1$. The arrows pointing right show the ε' behaviour when $\tilde{J}$ increases, and the arrows pointing left show the ε' behaviour when $\tilde{J}$ decreases. The vertical arrows point to the jumps between the lower and upper stable branches. The SP excitation is possible only below the horizontal thick line at $\varepsilon' = -1$.

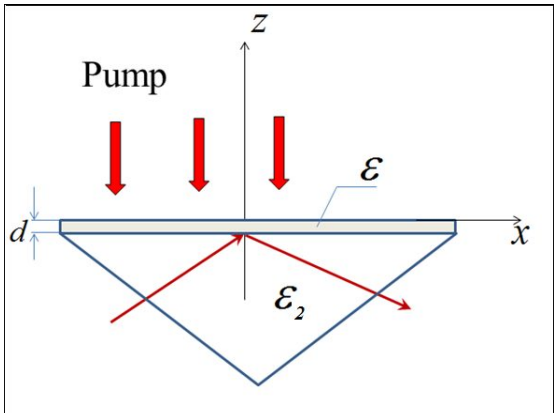

Figure 5. Experimental configuration. The organic film with the dielectric function ε depending on the pump (thick arrows) contacts the dielectric prism. SPs are excited with external weak p-polarized electromagnetic field (thin arrow) propagating in the dielectric prism (Kretschmann-Raether configuration[35]).

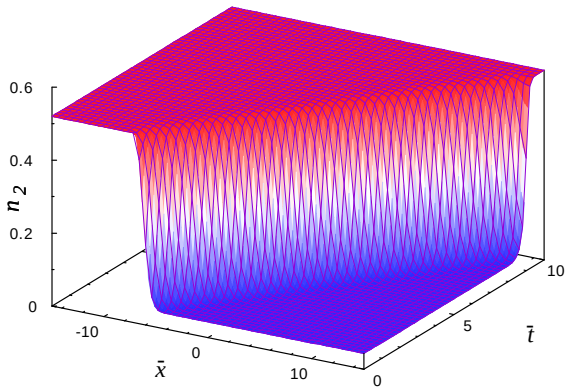

Figure 6. SW for $(\omega_{21}-\omega)/\sqrt{2\sigma_{2s}}=0.5$ and $J=2.4$ as a function of dimensionless coordinate $\bar{x}=x/\sqrt{DT_1}$ and time $\bar{t}=t/T_1$, where $\sqrt{DT_1}$ is the diffusion path length.

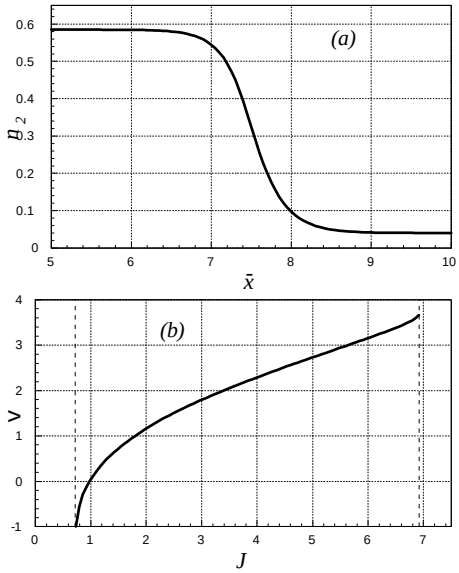

Figure 7. Instantaneous profile (a) at $J=6.91$ and velocities (b) of the SW. Detuning $(\omega_{21}-\omega)/\sqrt{2\sigma_{2s}}$ is equal to 0.25. The velocity is given in terms of $\bar{v}_{\max}$.

where D is the diffusional coefficient that can be expressed in terms of the strength of the near dipole-dipole interaction p

$$D=0.171\frac{p^2}{N^{2/3}}T' \tag{27}$$

Here T' is the irreversible dephasing time of the electronic transition.[16] The above mentioned steady-state spacely inhomogeneous distribution of the excited state population n_2 corresponding to the Maxwell value of the exciting radiation $\tilde{J}_M$ is the solution of steady-state diffusional equation, Eq.(26), when $\partial n_2/\partial t=0$. The SWs $n_2=n_2(x-vt)$ are the solutions of non-steady-state Eq.(26) for the boundary conditions at the edges of the sufficiently long, as compared with the width of SWs, organic film corresponding to the values of n_2 related to different branches of the function $n_2(\tilde{J})$ showing the bistable behaviour. They are displayed in Fig.6 for the values of parameters given in Section 2.2 that lead to $T'=2.5\cdot10^{-14}s$ and $D=6.7\ cm^2/s$. We have also checked that the diffusional approximation is correct.

Figs.7 and 8 show the profiles of SWs corresponding to maximal velocities, and the velocities as functions of the power density of the exciting radiation for $(\omega_{21}-\omega)/\sqrt{2\sigma_{2s}}=0.25$ (the bistability range $J=0.72-6.92$) and 0.5 (the bistability range $J=0.594-2.415$), respectively. The corresponding values of $\tilde{J}[\frac{photons}{cm^2s}]=J/(\sigma_aT_1)$ can

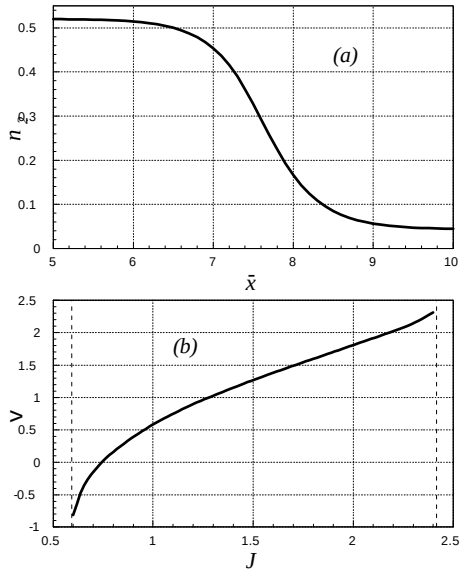

Figure 8. Instantaneous profile (a) at $J = 2.4$ and velocities (b) of the SW. Detuning $(\omega_{21} - \omega)/\sqrt{2\sigma_{2s}}$ is equal to 0.5. The velocity is given in terms of $\bar{v}_{\max}$.

be obtained by multiplying J by $10^{25}[\frac{photons}{cm^2 s}]$ for $\sigma_a \approx 10^{-16} cm^2$.[12] One can see the alternating-sign dependence of the switching wave velocity on pump intensity. Zero values of the SW velocities correspond to the Maxwell value of the exciting radiation $\tilde{J}_M$ ($= 0.978 \times 10^{25}[\frac{photons}{cm^2 s}]$ for Fig.7 and $0.743 \times 10^{25}[\frac{photons}{cm^2 s}]$ for Fig.8). If $\tilde{J} > \tilde{J}_M$, the SW moves right ($v > 0$). If $\tilde{J} < \tilde{J}_M$, the SW moves left ($v < 0$).

Using evaluations for the maximal velocity $\bar{v}_{\max} \simeq \sqrt{D/T_1}$ and for the wave front width $\sqrt{DT_1}$ of the SW,[19] one gets $\bar{v}_{\max} \simeq 8.2 \times 10^4$ cm/s and $\sqrt{DT_1} \simeq 8.2 \times 10^{-5} cm$ for the used values of the parameters where $T_1 = 10^{-9} s$. The transverse width of the thin film should be considerably larger than the wave front width, i.e. 1 μm. One can see that in reality the maximal velocity is nearly twice or triple as large as $\bar{v}_{\max}$.

As a mater of fact, in the case under consideration SW represents the wave of dramatic change of the dielectric permittivity of organic dye films (experimentally, the laser-induced change of the dielectric permittivity of dye nanoparticles of the order of unity observed in Ref.[15]). This may have many applications including addressing theoretical predictions of quantum field theory in time-dependent environments.[37]

Specifically, since only the lower branch of the bistability curve will correspond to the SP generation in linear regime (see above and Fig.4), the SWs offer the prospect of the optical manipulation of the SPs. Indeed, the range of existing the SPs in Figs.7 and 8 increases or decreases depending on whether the SW propagates to the left or the right. Moreover, because the wave number of the SP is equal to $k_x = \Omega/v_{SP} = \frac{\Omega}{c}\sqrt{\frac{\varepsilon(\Omega)\varepsilon_2}{\varepsilon_2+\varepsilon(\Omega)}}$ where $\varepsilon_2 > 0$ is the dielectric constant of an adjacent dielectric,[3,35] the SP velocity is given by $v_{SP} = c\sqrt{1/\varepsilon_2 + 1/\varepsilon(\Omega)}$. It dramatically slows down at resonance $\varepsilon(\Omega) \approx -\varepsilon_2$, and may be of the same order of magnitude as the velocity of the SW, $\bar{v}_{\max}$. In such a situation, one can speak, among other processes, about collisions between SPs and SWs.

Preliminary results of this section has been published in recent letter.[38]

4.1 Influence of SW on SP generation

To demonstrate the influence of the SW on the SP generation, we have carried out the corresponding calculations when the SW velocity is much smaller than that of the SPs by the finite-difference time-domain (FDTD) method. We used commercially available FDTD Solutions software by Lumerical.[39] Figs. 9, 10 and 11 show preliminary results demonstrating the influence of the SW, corresponding to bistability curve of Fig.4 for $y = 0.25$, on the SP generation, when the SW velocity is much smaller than that of the SPs. The experimental configuration is shown in Fig.5. The organic film of thickness 100 nm is found between silica substrate ($\varepsilon_s = 2.2$) and air,

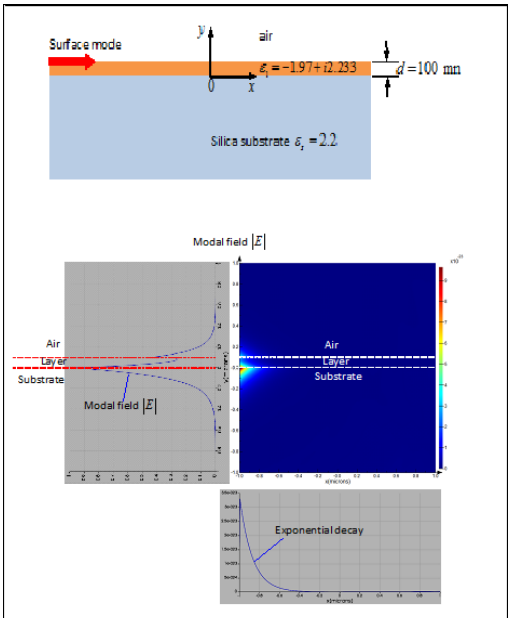

Figure 9. SPs in the absorbing film for the lower branch of the bistability curve ($n_2 \simeq 0.0016$, $\varepsilon = -1.97 + i2.233$) in the absence of SW.

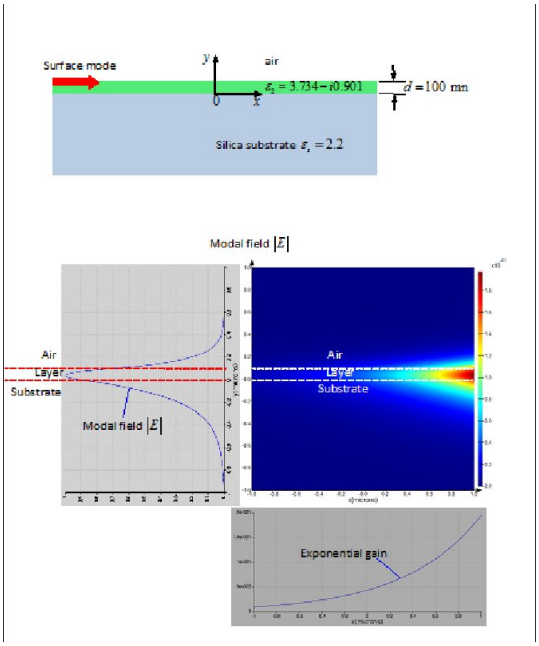

Figure 10. SPs in the amplifying film for the upper branch of the bistability curve ($n_2 = 0.4$, $\varepsilon = 3.734 - i0.901$) in the absence of SW.

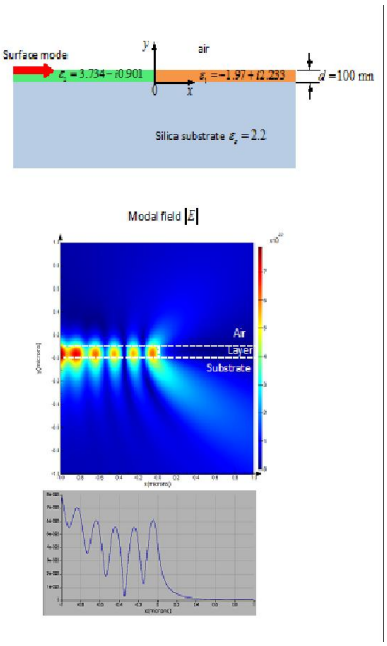

Figure 11. SPs in the organic film in the presence of SW when the SW velocity is much smaller than that of the SPs. The SW front is found at $x = 0$.

and is irradiated with a strong field of the power density of exciting radiation $\tilde{J} = 0.748 \times 10^{25}[\frac{photons}{cm^2 s}]$ (the corresponding dimensionless parameter $J = 0.748$). This results in the excited state population $n_2 \simeq 0.0016$ and the dielectric function $\varepsilon = -1.97 + i2.233$ for the lower branch; $n_2 = 0.4$ and $\varepsilon = 3.734 - i0.901$ (amplifying thin organic film) for the upper branch. Figs. 9 and 10 show the SP fields in the transverse and longitudinal directions for the lower and upper branches, respectively, in the absence of the SW. The fields decay in the transverse direction as the distance from the surfaces of the film increases. As to the longitudinal direction, the field decays exponentially in the absorbing film ($\varepsilon = -1.97 + i2.233$), Fig.9, and grows exponentially in the amplifying film ($\varepsilon = 3.734 - i0.901$), Fig.10. In the presence of the SW, if the SW front is found at $x = 0$, Fig.11, the SP propagating in the amplifying medium ($x < 0$), is reflected from the interface between amplifying and absorbing ($x > 0$) media at $x = 0$, resulting in the interference structure shown in Fig.11.

5. CONCLUSION

In this work we have developed a theory of nonlinear light-induced "plasmonic" properties of organic materials. Our consideration is based on the model of the interaction of strong shaped laser pulse with organic molecules, Ref.,[16] extended to the dipole-dipole intermolecular interactions in the condensed matter. We show that such a generalization can describe both a red shift of the resonance frequency of isolated molecules, according to the CMLL mechanism,[17] and the wide variations of their spectra related to the aggregation of molecules into J- or H-aggregates. In particular case of weak radiation we recover the CES approximation.[28–30] Our theory contains experimentally measured quantities that makes it closely related to experiment. The bistable response of organic materials in the condensed phase has been demonstrated using the electron-vibrational model. We predict the generation of the switching waves, or kinks in the bistable organic thin films that enable us to observe a bistable behaviour of the surface polaritons at the organic thin film/dielectric interface under the laser irradiation. We present the alternating-sign dependence of the switching wave velocity on pump intensity and discuss a possibility of controlling the polariton propagation by switching waves.

ACKNOWLEDGMENTS

We thank M. A. Noginov for useful discussions. We gratefully acknowledge support by the Action "Nonlinear Quantum Optics" (MP1403) of the European Cooperation in Science & Technology (COST).

6. APPENDIX A

In the case of the Gaussian modulation of the electronic transition by the vibrations, the absorption and fluorescence lineshapes are given by[20,21,33,40]

$$\begin{aligned} F_a(\omega) &= \frac{1}{\pi}\,\mathrm{Re}\int_0^\infty \exp[i(\omega-\omega_{21})t+g(t)]dt \\ F_f(\omega) &= \frac{1}{\pi}\,\mathrm{Re}\int_0^\infty \exp[i(\omega-\omega_{21}+\omega_{st})t+g^*(t)]dt \end{aligned} \tag{28}$$

where

$$g(t) = -\int_0^t dt'(t-t')K(t') \tag{29}$$

is the logarithm of the characteristic function of the spectrum of single-photon absorption after substraction of a term which is linear with respect to t and determines the first moment of the spectrum, $K(t)$ is the correlation function. If the latter is real,

$$W_{a(f)}(\omega) = \frac{1}{\pi}\int_0^\infty \exp[i(\omega-\omega_{21}+\delta_{a(f),f}\omega_{st})t+g(t)]dt \tag{30}$$

For the exponential correlation function $K(t) = \sigma_{2s}\exp(-|t|/\tau_s)$, we get

$$g(t) = -\sigma_{2s}\tau_s^2[\exp(-t/\tau_s)+\frac{t}{\tau_s}-1] \tag{31}$$

that gives Eq.(21) of section 2.2.

7. APPENDIX B

7.1 Switching waves

For the steady-state conditions, Eq.(24) becomes $F(n_2)=0$. Then it represents the balance of the excited state population for stationary and transversely homogeneous distributions and has two stable solutions under the bistability conditions. Let us denote the solutions corresponding to the maximum and minimum population as $n_{2,\max}$ and $n_{2,\min}$, respectively. They correspond to the upper and lower branches of the function $n_2(J)$. The SWs, or kinks are non-steady-state and transversely inhomogeneous distributions of population depending on the combination of time t and coordinate x, $\xi = x - vt$, propagating with the constant velocity v. They are given by the solutions of the ordinary differential equation following from Eq.(26) of the main text

$$D\frac{d^2n_2}{d\xi^2} + v\frac{dn_2}{d\xi} - F(n_2) = 0 \tag{32}$$

with the boundary conditions

.

$$n_2(\xi\to-\infty) = n_{2,\max}, \quad n_2(\xi\to+\infty) = n_{2,\min} \tag{33}$$

Inversion of the boundary conditions, Eq.(33), is equivalent to changing the sign of the velocity v. We do not specify here how such a population distribution was created. For example, one can use additional illumination of varying intensity that acts at $t<0$. Its intensity diminishes from larger values to obtain population $n_{2,\max}$, and increases from small values to obtain population $n_{2,\min}$. This issue will be discussed in more details elsewhere.

SWs exist in the domain of bistability of homogeneous steady-state distributions. Important special case is the motionless SW with zero velocity $v=0$. Then $\xi = x$, and Eq.(32) is reduced to the Newtonian equation for one-dimensional motion of a mechanical point particle under the action of "force" F:

$$D\frac{d^2n_2}{dx^2} = F(n_2) \tag{34}$$

where coordinate x plays the role of "time". The corresponding "potential energy" is

$$U(n_2) = -\int^{n_2} F(n_2')dn_2', \tag{35}$$

and the conservation law of "mechanical energy" W, which is the sum of the "kinetic" and "potential" energy, reads

$$\frac{dW}{dx} = 0 \tag{36}$$

where

$$W = \frac{D}{2}(\frac{dn_2}{dx})^2 + U(n_2) \tag{37}$$

The "potential" is represented by a two-hump curve in the bistability domain and by a single-hump curve outside it. The motionless SW (with $v = 0$) corresponds to the two humps of the same height, $U(n_{2\,\max}) = U(n_{2\,\min})$, or to the "Maxwell's rule" (according to the terminology of the theory of phase transitions of the first kind)

.

$$\int_{n_{2\,\min}}^{n_{2\,\max}} F(n_2)dn_2 = 0 \tag{38}$$

For moving (in the direction x that is perpendicular to the pump radiation propagation) SWs, the "energy" W is not constant:

$$\frac{dW}{d\xi} = -v(\frac{dn_2}{d\xi})^2$$

Correspondingly, the "energy" varies monotonically in the whole interval $-\infty < \xi < \infty$, and one can show that also the population n_2 behaves in a similar manner. Examples of SWs profiles are given in Figs. 6, 7, 8 of the main text. The SWs knowledge allows one to find the spatial bistability (two different shapes of distributions $n_2(x)$ for the excitation by a wide beam of pump) and spatial hysteresis (dynamics of these distributions with slow increase and decrease of the pump power). For pump profiles including a number of maxima, e.g., for periodic in x pump intensity, soliton-like population distributions can be formed promising for information storage with molecular data-recording devices. SWs were introduced and studied in optics in Ref.;[18] more information on SWs can be found in monograph.[19]

7.2 Expressing diffusion coefficient in terms of the strength of near dipole-dipole interaction

The diffusion coefficient can be written in the form (see Eq.(2.54) of Ref.[36])

$$D = \frac{1}{3}\frac{R_{0D}^6}{T_1\bar{R}^4} \tag{39}$$

where $\bar{R}$ is the average distance between donors ($(4/3)\pi\bar{R}^3 = 1/N$), N is the density of donors (molecules), R_{0D} is the Forster critical distance for the excitation energy transfer, T_1 is the excited state lifetime in the absence of the transfer. R_{0D} may be evaluated from the condition that the dimensionless parameter determining the transfer rate $2\hbar^{-2}|M_{12}|^2T_2\tau_0$ is of the order of 1:[36]

$$2\hbar^{-2}|M_{12}|^2T'T_1 \sim 1 \tag{40}$$

Here T' is the irreversible dephasing time of the electronic transition,

$$|M_{12}|^2 = \frac{2}{3}\frac{|D_{12}|^4}{R_{0D}^6} \tag{41}$$

is the square of the matrix element of the dipole-dipole interaction where $|D_{12}|^4$ can be expressed in terms of the strength of the near dipole-dipole interaction p (see the main paper) as

$$|D_{12}|^4 = \frac{9\hbar^2}{16\pi^2}\frac{p^2}{N^2} \tag{42}$$

Using Eqs.(39)-(42), one gets Eq.(27) of the main text.

The diffusional approximation is correct when $\tau << T_1$[36] where τ is the average lifetime of the excitation at a donor with $\tau^{-1} = T_1^{-1}\left(\frac{R_{0D}}{R}\right)^6$. This gives

$$T_1/\tau = \frac{4}{3}p^2 T' T_1, \tag{43}$$

using Eqs.(**??**)-(42). For the values of parameters $p \simeq 4 \cdot 10^{14}\ s^{-1}$, $T' = 2.5 \cdot 10^{-14}\ s$ and $T_1 = 10^{-9}\ s$ (see the main paper), we obtain $T_1/\tau >> 1$, i.e. the diffusional approximation is correct.

7.3 Evaluations of maximal switching wave velocity and wave front width

The diffusion length l_{diff} is related to the diffusional coefficient D by the well-known equation $l_{diff} = \sqrt{D\tau_{exc}}$, where τ_{exc} is the excitation lifetime. In our case T_1 plays the role of τ_{exc}. The switching wave velocity can be evaluated by $v \simeq l_{diff}/\tau_{rel}$[19] where $\tau_{rel} \sim T_1$ is the time of the establishment of the nonlinearity. So, one can easily obtain the evaluation for the maximal switching wave velocity $\bar{v}_{\max} \simeq \sqrt{D/T_1}$ below Fig.8. As to the wave front width, it may be evaluated as $l_{diff} = \sqrt{DT_1}$.

REFERENCES

1. M. Durach, A. Rusina, V. I. Klimov, and M. I. Stockman, "Nanoplasmonic renormalization and enhancement of coulomb interactions," *New J. of Phys.* **10**, p. 105011, 2008.
2. N. J. Halas, S. Lal, W.-S. Chang, S. Link, and P. Nordlander, "Plasmons in strongly coupled metallic nanostructures," *Chem. Rev.* **111**, pp. 3913–3961, 2011.
3. S. A. Maier, *Plasmonics: Fundamentals and Applications*, Springer, New York, 2007.
4. U. Leonhardt and T. Philbin, *Geometry and Light. The Science of Invisibility*, Dover Publications, Mineola, New York, 2010.
5. J. B. Khurgin, "How to deal with the loss in plasmonics and metamaterials," *Nature Nanotechnology* **10**, pp. 2–6, 2015.
6. A. J. Hoffman, L. Alexeev, S. S. Howard, K. J. Franz, D. Wasserman, V. A. Podolskiy, E. E. Narimanov, D. L. Sivco, and C. Gmachl, "Negative refraction in semiconductor metamaterials," *Nature Materials* **6**, pp. 946–950, 2007.
7. F. H. L. Koppens, D. E. Chang, and F. J. G. de Abajo, "Graphene plasmonics: A platform for strong light-matter interaction," *Nano Letters* **11**, pp. 3370–3377, 2011.
8. J. Chen, M. Badioli, P. Alonso-Gonzalez, S. Thongrattanasiri, F. Huth, J. Osmond, M. Spasenovic, A. Centeno, A. Pesquera, P. Godignon, A. Z. Elorza, N. Camara, F. J. G. de Abajo, R. Hillenbrand, and F. H. L. Koppens, "Optical nano-imaging of gate-tunable graphene plasmons," *Nature* **487**, pp. 77–81, 2012.
9. Z. Fei, A. S. Rodin, G. O. Andreev, W. Bao, A. S. McLeod, M. Wagner, L. M. Zhang, Z. Zhao, M. Thiemens, G. Dominguez, M. M. Fogler, A. H. C. Neto, C. N. Lau, F. Keilmann, and D. N. Basov, "Gate-tuning of graphene plasmons revealed by infrared nano-imagine," *Nature* **487**, pp. 82–85, 2012.
10. L. Gu, J. Livenery, G. Zhu, E. E. Narimanov, and M. A. Noginov, "Quest for organic plasmonics," *Applied Phys. Lett.* **103**, p. 021104, 2013.
11. M. J. Gentile, S. Nunez-Sanchez, and W. L. Barnes, "Optical field-enhancement and subwavelength field-confinement using excitonic nanostructures," *Nano Letters* **14**, pp. 2339–2344, 2014.
12. B. D. Fainberg and G. Li, "Nonlinear organic plasmonics: Applications to optical control of coulomb blocking in nanojunctions," *Applied Phys. Lett.* **107**(5), p. 053302, 2015. [Erratum, v. 107, 109902 (2015)].

13. G. Li, M. S. Shishodia, B. D. Fainberg, B. Apter, M. Oren, A. Nitzan, and M. Ratner, "Compensation of coulomb blocking and energy transfer in the current voltage characteristic of molecular conduction junctions," *Nano Letters* **12**, pp. 2228–2232, 2012.
14. A. J. White, B. D. Fainberg, and M. Galperin, "Collective plasmon-molecule excitations in nanojunctions: Quantum consideration," *J. Phys. Chem. Lett.* **3**, pp. 2738–2743, 2012.
15. T. U. Tumkur, J. K. Kitur, L. Gu, G. Zhu, and M. A. Noginov, "Gigantic optical nonlinearity: Laser-induced change of dielectric permittivity of the order of unity," *ACS Photonics* **2**, pp. 622–627, 2015.
16. B. D. Fainberg, "Nonperturbative analytic approach to interaction of intense ultrashort chirped pulses with molecules in solution: Picture of "moving" potentials," *J. Chem. Phys.* **109**(11), pp. 4523–4532, 1998.
17. M. V. Klein and T. E. Furtak, *Optics*, Willey, New York, 1988.
18. N. N. Rosanov *Sov. Phys. JETP* **53**, p. 47, 1981.
19. N. N. Rosanov, *Spatial Hysteresis and Optical Patterns*, Springer, Berlin, 2002.
20. B. D. Fainberg in *Advances in Multiphoton Processes and Spectroscopy*, S. H. Lin, A. A. Villaeys, and Y. Fujimura, eds., **15**, pp. 215–374, World Scientific, Singapore, New Jersey, London, 2003.
21. S. Mukamel, *Principles of Nonlinear Optical Spectroscopy*, Oxford University Press, New York, 1995.
22. B. D. Fainberg *Opt. Spectrosc.* **68**, p. 305, 1990. [Opt. Spektrosk., vol. 68, 525, 1990].
23. B. Fainberg *Phys. Rev. A* **48**, p. 849, 1993.
24. B. D. Fainberg, "Non-linear polarization and spectroscopy of vibronic transitions in the field of intensive ultrashort pulses," *Chem. Phys.* **148**, pp. 33–45, 1990.
25. A. S. Davydov, *Theory of Molecular Excitons*, Plenum, New York, 1971.
26. B. D. Fainberg and B. Levinsky, "Stimulated raman adiabatic passage in a dense medium," *Adv. Phys. Chem.* **2010**, p. 798419, 2010.
27. M. E. Crenshow, M. Scalora, and C. M. Bowden, "Ultrafast intrinsic optical switching in dense medium of two-level atoms," *Phys. Rev. Lett.* **68**, pp. 911–914, 1992.
28. A. Eisfeld and J. S. Briggs, "The j-band of organic dyes: lineshape and coherence length," *Chem. Phys.* **281**, pp. 61–70, 2002.
29. A. Eisfeld and J. S. Briggs, "The j- and h-bands of organic dye aggregates," *Chem. Phys.* **324**, pp. 376–384, 2006.
30. A. Eisfeld and J. S. Briggs, "Absorption spectra of quantum aggregates interacting via long-range forces," *Phys. Rev. Lett.* **96**, p. 113003, 2006.
31. M. Abramowitz and I. Stegun, *Handbook on Mathematical Functions*, Dover, New York, 1964.
32. S. G. Rautian and I. I. Sobel'man, "The effect of collisions on the doppler broadening of spectral lines," *SOVIET PHYSICS USPEKHI* **9**(5), pp. 701–716, 1967. [Usp. Fiz. Nauk 90, 209-238 (1966)].
33. B. D. Fainberg *Opt. Spectrosc.* **58**, p. 323, 1985. [Opt. Spektrosk. v. 58, 533 (1985)].
34. N. N. Bogoliubov and Y. A. Mitropolskyi, *Asymptotic methods in the theory of non-linear oscillations*, Gordon and Breach, New York, 1961.
35. H. Raether, *Surface Plasmons on Smooth and Rough Surfaces and on Gratings*, Springer-Verlag, Berlin, 1986.
36. V. M. Agranovich and M. D. Galanin, *Electronic Excitation Energy Transfer in Condensed Matter*, North-Holland, Amsterdam, New York, 1983.
37. D. Faccio, A. Prain, N. Westerber, S. Vezzol, and T. Roger in *Abstracts of NANOMETA 2017*, pp. sat5o–2, Seefeld, Austria, 2017.
38. B. D. Fainberg, N. N. Rosanov, and N. A. Veretenov, "Light-induced "plasmonic" properties of organic materials: Surface polaritons and switching waves in bistable organic thin films," *Applied Phys. Lett.* **110**, p. 203301, 2017.
39. http://www.lumerical.com/, *Lumerical Solutions*, Inc.: Vancouver, B.C., Canada.
40. R. Kubo, "Relaxation, fluctuation and resonance in magnetic systems," p. 23, Oliver Boyd, Edinburgh, 1962.